



## Short communication

## Low-cost method for sodium borohydride regeneration and the energy efficiency of its hydrolysis and regeneration process

L.Z. Ouyang<sup>a, b, c</sup>, H. Zhong<sup>a, b</sup>, Z.M. Li<sup>a, b</sup>, Z.J. Cao<sup>a, b</sup>, H. Wang<sup>a, b</sup>, J.W. Liu<sup>a, b</sup>, X.K. Zhu<sup>a, b</sup>, M. Zhu<sup>a, b, \*</sup><sup>a</sup> School of Materials Science and Engineering, South China University of Technology, Guangzhou 510641, People's Republic of China<sup>b</sup> Key Laboratory of Advanced Energy Storage Materials of Guangdong Province, South China University of Technology, Guangzhou 510641, People's Republic of China<sup>c</sup> Key Laboratory for Fuel Cell Technology in Guangdong Province, South China University of Technology, Guangzhou 510641, People's Republic of China

## H I G H L I G H T S

- The regeneration process for NaBH<sub>4</sub> is designed using MgH<sub>2</sub> with NaBO<sub>2</sub>.
- The energy efficiency of the hydrolysis and regeneration of NaBH<sub>4</sub> is 49.91%.
- A cheap method for NaBH<sub>4</sub> regeneration was developed by reacting H–Mg<sub>3</sub>La with NaBO<sub>2</sub>.
- The mechanism of NaBH<sub>4</sub> regeneration by reacting Mg<sub>3</sub>La hydride with NaBO<sub>2</sub> is revealed.

## A R T I C L E I N F O

## Article history:

Received 8 March 2014

Received in revised form

8 July 2014

Accepted 12 July 2014

Available online 18 July 2014

## Keywords:

Sodium borohydride

Energy efficiency

Magnesium–lanthanum hydrides

Ball milling

## A B S T R A C T

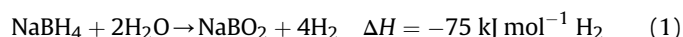
Hydrolysis of sodium borohydride (NaBH<sub>4</sub>) is one of the most attractive methods for energy generation of mobile systems used as hydrogen source because of the high gravimetric density and controllable hydrogen generation of NaBH<sub>4</sub>. However, regeneration of NaBH<sub>4</sub> is a key issue that remains to be solved, and the energy efficiency of NaBH<sub>4</sub> is unknown. In the present study, the energy efficiency of NaBH<sub>4</sub> hydrolysis and the entire process of sodium metaborate (NaBO<sub>2</sub>) regeneration via reaction with magnesium hydride (MgH<sub>2</sub>) is determined through thermodynamics calculations. The maximum energy efficiency is 49.91%, indicating that NaBH<sub>4</sub> generation by reaction between MgH<sub>2</sub> and NaBO<sub>2</sub> during ball milling is feasible. An inexpensive high-energy ball milling method is employed to regenerate NaBH<sub>4</sub> by reaction of NaBO<sub>2</sub> with magnesium–lanthanum hydrides (H–Mg<sub>3</sub>La). Products after ball milling are characterized through Fourier transform infrared spectroscopy and X-ray diffraction measurements. In the reaction of NaBO<sub>2</sub> with H–Mg<sub>3</sub>La, MgH<sub>2</sub> reacts with NaBO<sub>2</sub> and then lanthanum hydride (LaH<sub>3</sub>) reacts with NaBO<sub>2</sub> to produce NaBH<sub>4</sub>.

© 2014 Elsevier B.V. All rights reserved.

## 1. Introduction

Because of the world energy crisis, replacement of fossil fuel has become a key issue. In this regard, hydrogen energy is an important alternative source of energy [1]. Unlike oil or natural gas, however, hydrogen is an energy carrier rather than a source of energy [2]. Appropriate methods for hydrogen generation and storage must therefore be developed to utilize it [3]. Hydrolysis is one of the most attractive methods of hydrogen generation because it obviates

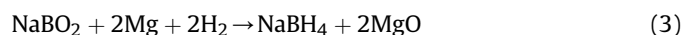
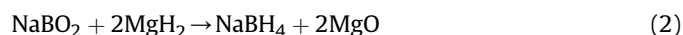
storage and produces a large amount of hydrogen. Among the hydrogen complexes that produce hydrogen by hydrolysis and function as storage material for hydrogen, sodium borohydride (NaBH<sub>4</sub>) has been extensively studied. It has been utilized in hydrogen supply systems of fuel cells [4,5]. The nonhazardous characteristic and high gravimetric density (10.8wt%) [3] of NaBH<sub>4</sub> favor the use of this complex in hydrogen production. NaBH<sub>4</sub> hydrolyzes according to the following process:



This highly controllable reaction generates pure hydrogen. Thus, it can be directly used in fuel cells [3,6]. The byproduct of this reaction, sodium metaborate (NaBO<sub>2</sub>), is environmentally friendly

\* Corresponding author. School of Materials Science and Engineering, South China University of Technology, Guangzhou 510641, People's Republic of China.  
E-mail address: [memzhu@scut.edu.cn](mailto:memzhu@scut.edu.cn) (M. Zhu).

and nontoxic. As  $\text{NaBH}_4$  hydrolysis is irreversible, a key issue is discovering a means to convert  $\text{NaBO}_2$  back to  $\text{NaBH}_4$  [7]. For example, the less-expensive reducing metal, magnesium (or its hydride), has been used to produce  $\text{NaBH}_4$  from dehydrated  $\text{NaBO}_2$ . Work on this approach was largely conducted by Kojima et al. [8]. They synthesized  $\text{NaBH}_4$  by heating a mixture of dehydrated  $\text{NaBO}_2$  and  $\text{MgH}_2$  or a mixture of  $\text{NaBO}_2$  and  $\text{Mg}$  under high  $\text{H}_2$  pressure and elevated temperature. This synthesis proceeds through reactions described in Equations (2) and (3).



Other researchers further studied processes for converting  $\text{NaBO}_2$  back to  $\text{NaBH}_4$  through the above reaction [10,11]. Kojima et al. [8] synthesized  $\text{NaBH}_4$  by heating dehydrated  $\text{NaBO}_2$  and magnesium silicide ( $\text{Mg}_2\text{Si}$ ) under high  $\text{H}_2$  pressure at elevated temperature. However, energy consumption of such processes is very high. To achieve a new, economical route of  $\text{NaBH}_4$  synthesis, Hsueh et al. [7], Çetin et al. [9], and Kong et al. [6] ball-milled dehydrated  $\text{NaBO}_2$  and  $\text{MgH}_2$  at room temperature. The yield of this process is 76%.

The U.S. Department of Energy advises against the use of  $\text{NaBH}_4$  in on-board automotive hydrogen storage. One of the main reasons behind this advisory is the cost of  $\text{NaBH}_4$  and the irreversible process of its hydrolysis [12]. We thus examined the energy efficiency and heat effect of the entire process of  $\text{NaBH}_4$  recycling to determine the feasibility of hydrogen generation by  $\text{NaBH}_4$  hydrolysis.  $\text{NaBO}_2$  and  $\text{MgH}_2$  were used to synthesize  $\text{NaBH}_4$  by ball milling, and the energy efficiency of the entire recycling process was determined through thermodynamic calculations. The energy consumption of the regeneration procedure was discussed in accordance with the calculations. To reduce the cost and temperature of  $\text{NaBH}_4$  synthesis, we reacted  $\text{MgH}_2$  and lanthanum hydride ( $\text{LaH}_3$ ) mixtures produced by hydrogenating magnesium–lanthanum alloy ( $\text{Mg}_3\text{La}$ ) [13–15] with  $\text{NaBO}_2$  by ball milling at room temperature. Our process avoids the use of  $\text{MgH}_2$ , which is synthesized by hydrogenation at a high temperature; it is thus an alternative route for the regeneration of  $\text{NaBH}_4$  for industrial use.

## 2. Experimental

### 2.1. Sample preparation

$\text{MgH}_2$  powder (98% purity) was purchased from Alfa Aesar (USA).  $\text{Mg}_3\text{La}$  was prepared by induction melting of  $\text{Mg}$  (99.9%) and lanthanum (99.9%) in an alumina crucible under an argon atmosphere. The alloys were milled for 0.5 h in a QM-2SP planetary ball mill at a ball-to-powder mass ratio of 20:1. The  $\text{NaBO}_2$  powder was dried at  $280^\circ\text{C}$  to obtain anhydrous  $\text{NaBO}_2$ . To prevent samples and raw materials from oxidation and/or hydroxide formation, they were stored and handled in an Ar-filled glove box equipped with a recirculation system.

### 2.2. Synthesis of $\text{NaBH}_4$

Hydrogenation of  $\text{Mg}_3\text{La}$  was performed for 0.5 h at room temperature.  $\text{MgH}_2$ – $\text{NaBO}_2$  mixtures (2:1 mole ratio) and magnesium hydride–lanthanum hydride ( $3\text{MgH}_2$ – $\text{LaH}_3$ )– $\text{NaBO}_2$  mixtures (4.4:9 mole ratio) were prepared. The mixtures were processed in a high-speed vibrating mill (QM-3C) using two sizes of balls.

### 2.3. Purification of $\text{NaBH}_4$

Purification of  $\text{NaBH}_4$  was accomplished by extracting  $\text{NaBH}_4$  with anhydrous ethylenediamine (99% purity) from the products after milling and then separating the extracted solution from the byproducts and remaining reactants through a polytetrafluoroethylene filter. The filtrate was dried in a vacuum oven at  $50^\circ\text{C}$  to obtain  $\text{NaBH}_4$ .

### 2.4. Sample characterization

H– $\text{Mg}_3\text{La}$ , as well as products after reaction and after purification were characterized by using a Philips X'Pert MPD X-ray diffractometer with Cu K $\alpha$  radiation. Patterns in the  $2\theta$  range of  $10^\circ$ – $90^\circ$  were recorded at a scanning rate of  $0.02^\circ\text{s}^{-1}$ . The reaction products were analyzed by Fourier transformed infrared (FT-IR) spectroscopy (Bruker Vector33).

## 3. Results and discussion

### 3.1. Regeneration of $\text{NaBH}_4$ using $\text{NaBO}_2$ and $\text{MgH}_2$

To obtain a cyclical process with  $\text{NaBH}_4$  hydrolysis and regeneration for hydrogen generation,  $\text{NaBH}_4$  was regenerated by using  $\text{NaBO}_2$  and  $\text{MgH}_2$ . Fig. 1 presents X-ray diffraction (XRD) patterns of the products after ball milling for different durations. Peaks of the XRD pattern of the product after 0.5 h of ball milling (Fig. 1(a)) could be indexed to  $\text{MgH}_2$ ,  $\text{NaBH}_4$  [16], and  $\text{MgO}$ . According to the phase analysis mentioned above,  $\text{NaBH}_4$  and the by-product  $\text{MgO}$  were produced after 0.5 h of ball milling. Peaks of the XRD pattern of the product after 2 h of ball milling (Fig. 1(c)) could be indexed to  $\text{NaBH}_4$  and  $\text{MgO}$ . In contrast to the XRD patterns in Fig. 1(a) and (b), the pattern in Fig. 1(c) does not have diffraction peaks of  $\text{MgH}_2$ . Stronger diffraction peaks of  $\text{NaBH}_4$  in Fig. 1(c) compared with peaks in Fig. 1(d) suggest that part of the  $\text{MgH}_2$  phase reacted with  $\text{NaBO}_2$  and part of it became refined. Peaks of the XRD pattern of the product after 4 h of ball milling (Fig. 1(e)) could be indexed to  $\text{NaBH}_4$  and  $\text{MgO}$ . The energy input for the vibrating mill used in this process of  $\text{NaBH}_4$  regeneration was omitted in the subsequent calculation.

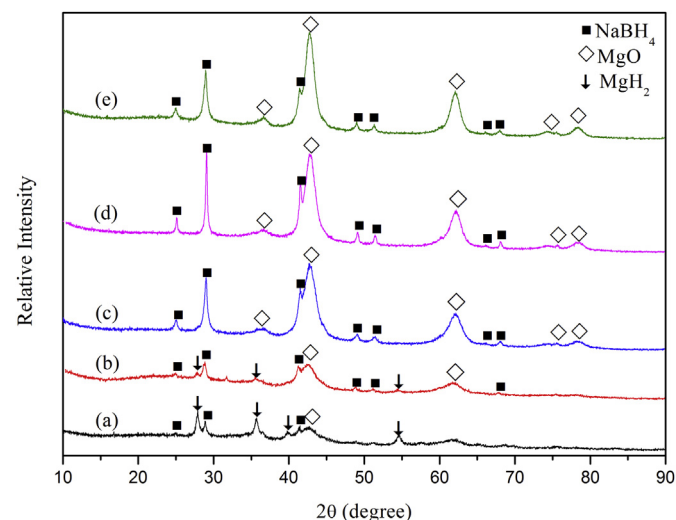


Fig. 1. XRD patterns of the powders produced after shaker milling the  $\text{MgH}_2$ – $\text{NaBO}_2$  mixture (in 2:1 mol ratio) for different durations (a) 30 min (b) 1 h (c) 2 h (d) 3 h (e) 4 h.

### 3.2. Energy efficiency of NaBH<sub>4</sub> hydrolysis and regeneration

Calculation of the energy efficiency of NaBH<sub>4</sub> hydrolysis and regeneration was based on the synthesis of NaBH<sub>4</sub> from MgH<sub>2</sub> and anhydrous NaBO<sub>2</sub>. The feasibility of this regeneration process was discussed according to the calculation results. Fig. 2 shows the cycle of NaBH<sub>4</sub> hydrolysis and regeneration of NaBH<sub>4</sub> and MgH<sub>2</sub>. The energy efficiency is confirmed by the ratio of energy output ( $E_o$ ) of the cycle to the energy ( $E_i$ ) input for the reaction of the cycle.

To calculate the energy efficiency, the cycle was divided into three parts. First, NaBH<sub>4</sub> in contact with ruthenium catalyst hydrolyzes at room temperature [17], as described in Equation (1). Through a reaction described in Equation (4), the hydrogen generated from this process can be used in a fuel cell.



Second, the byproduct NaBO<sub>2</sub> reacts with MgH<sub>2</sub> during ball milling, producing NaBH<sub>4</sub> and the byproduct MgO (Equation (2)), and NaBH<sub>4</sub> could then be purified with ethylenediamine and the products could be separated. In order to recycle the byproduct MgO, a method to produce MgH<sub>2</sub> from MgO should be found. This requirement is met by Mg, which is produced industrially by electrolysis of fused magnesium chloride (Equations (5) and (6)) in the third step:



Here, chlorine is used to react with MgO at 900 °C to produce MgCl<sub>2</sub>, and Mg is obtained by electrolysis of fused MgCl<sub>2</sub>. Mg obtained from Equation (6) may be hydrogenated to produce MgH<sub>2</sub> according to Equation (7) [18]:



The energy from the exothermic hydrogenation could be stored and utilized for other purposes. MgH<sub>2</sub> produced in this process can react with NaBO<sub>2</sub> again to produce NaBH<sub>4</sub>.

For convenience, all of the aforementioned reactions are assumed to proceed at constant pressure, and the fuel cell reaction is assumed to occur at constant temperature and pressure. We based the calculation on the assumption that the entire cycle is an ideal path, which means that the extent of reactions is 100% and that all products are completely separated.

**Table 1**

Enthalpy change of each reaction in the cycling.

Number (i)	Reaction	Enthalpy change (kJ mol <sup>-1</sup> )
1	$\text{H}_2 + 1/2\text{O}_2 \rightarrow \text{H}_2\text{O}$	$\Delta H_1 = -285.83$
2	$1/4\text{NaBH}_4 + 1/2\text{H}_2\text{O} \rightarrow 1/4\text{NaBO}_2 + \text{H}_2$	$\Delta H_2 = -75.00$
3	$1/4\text{NaBO}_2 + 1/2\text{MgH}_2 \rightarrow 1/4\text{NaBH}_4 + 1/2\text{MgO}$	$\Delta H_3 = -65.87$
4	$1/2\text{MgO} + 1/2\text{Cl}_2 \rightarrow 1/4\text{O}_2 + 1/2\text{MgCl}_2 (900^\circ\text{C})$	$\Delta H_4 = -35.26$
5	$1/2\text{MgCl}_2 \rightarrow 1/2\text{Cl}_2 + 1/2\text{Mg} (710^\circ\text{C})$	$\Delta H_5 = 298.79$
6	$1/2\text{Mg} + 1/2\text{H}_2 \rightarrow 1/2\text{MgH}_2$	$\Delta H_6 = -76.15$

According to the standards database [19], the standard enthalpy change of these reactions can be computed as follows:

$$\Delta_r H_m = \sum n \Delta_f H_m \quad (8)$$

where,  $\Delta_r H_m$  is the standard enthalpy of reaction,  $n$  is the stoichiometric number of each reaction component, and  $\Delta_f H_m$  is the standard enthalpy of formation. Therefore, the enthalpy change of the reaction may be computed through Kirchhoff's formula:

$$\Delta H_m = \Delta_r H_m + \int C_p dT \quad (9)$$

where,  $\Delta H_m$  is the enthalpy of reaction,  $C_p$  is the heat capacity at constant pressure, and  $T$  is the absolute temperature. Because all of the reactions proceed at constant pressure, the thermal effect of the reaction is equivalent to enthalpy change.

In the cycle, the energy released by the exothermic reaction may be collected for recycling. This part of the energy is thus ignored in the calculation and is regarded as heat released from the reaction. However, energy that the endothermic reaction absorbs is the energy input from the environment, which may be computed from the enthalpy change.

The Gibbs free energy is the maximum amount of non-expansion work that can be extracted from the reaction at constant temperature and pressure [20]. Hydrogen reacts with oxygen in fuel cells at constant temperature and pressure, resulting in energy release; thus, the Gibbs free energy of this reaction is the maximum amount of energy that can be extracted. The standard Gibbs free energy of water is the maximum amount of  $E_o$  of the cycle. The energy efficiency ( $\eta$ ) of NaBH<sub>4</sub> hydrolysis and regeneration is thus given by the formula:

$$\eta = E_o/E_i \quad (10)$$

To standardize the unit of measure, the stoichiometric amount of reactants is determined by the number required to generate of 1 mole of hydrogen. For example, 1/4 mole of NaBH<sub>4</sub> as reactant can produce 1 mole of H<sub>2</sub>, according to Equation (1); thus, the stoichiometric number of NaBH<sub>4</sub> is 1/4.

Table 1 shows the enthalpy change of each reaction in the cycle. Equation (7) describes the endothermic reaction of this cycle.

However, purification of NaBH<sub>4</sub> entails the evaporation of ethylenediamine, which is endothermic. The enthalpy of vaporization that generates 1 mole of hydrogen is 33.34 kJ, here referred to as  $\Delta H_7$ .

According to Fig. 2, hydrogen used to produce MgH<sub>2</sub> could not be regenerated in this cycle. Therefore, additional energy input into the cycle is due to hydrogen, and  $E_i$  is described by Equation (11):

$$E_i = |1/2\Delta H_1| + \Delta H_5 + \Delta H_7 = 475.05 \text{ kJ} \quad (11)$$

where,  $\Delta H_1$  is the enthalpy of Equation (4), and  $\Delta H_5$  is the enthalpy of Equation (6).

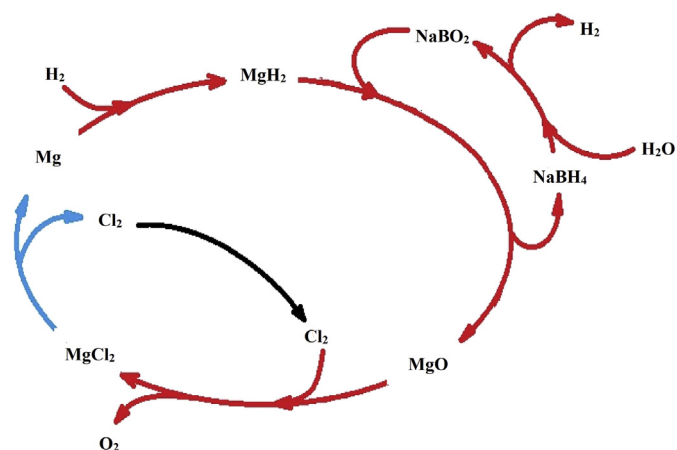
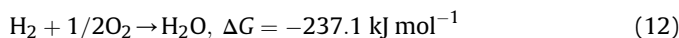


Fig. 2. The path of NaBH<sub>4</sub> hydrolysis cycling.

The Gibbs free energy of the reaction between  $H_2$  and  $O_2$  is  $-237.1 \text{ kJ mol}^{-1}$ , according to Equation (12):



$E_o$  of the cycle is also the Gibbs free energy ( $\Delta G$ ) from Equation (12).  $E_o$  is expressed as follows:

$$E_o = |\Delta G| = 237.1 \text{ kJ} \quad (13)$$

According to Equation (10), the maximum energy efficiency is 49.91%, indicating that about half of the  $E_i$  in the cycle is the output in each cycle. If the heat released by the exothermic reaction can be collected for recycling, then the maximum energy efficiency is further improved. It was reported that MgO could be reduced to Mg in a solar furnace [21], which is environmentally friendly and is able to improve the maximum energy efficiency. Therefore, according to the maximum energy efficiency that was computed, the cycle is feasible.

### 3.3. Synthesis of $NaBH_4$ using $H-Mg_3La$

Hydrogenation using Mg is relatively difficult, but  $Mg_3La$  easily undergoes hydrogenation at room temperature. In contrast to the method that uses  $MgH_2$  to produce  $NaBH_4$ , regeneration by  $H-Mg_3La$  may reduce the energy consumption. Therefore, we used  $H-Mg_3La$  and  $NaBO_2$  to regenerate  $NaBH_4$  by ball milling. Fig. 3 shows the XRD pattern of hydrogenated  $Mg_3La$ . The peaks could be indexed to  $MgH_2$ ,  $LaH_3$  and  $MgO$ , the last of which was found in small amounts. These results indicate that the  $Mg_3La$  phase reacted with hydrogen and transformed into  $MgH_2$  and  $LaH_3$ , and that production of  $MgO$  was due to the oxidization of  $Mg_3La$ . The reaction may be described as follows:

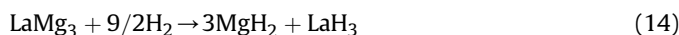


Fig. 4(a) shows the XRD patterns of the reactant mixture before ball milling. Its peaks could be indexed to  $LaH_3$ ,  $NaBO_2$ ,  $MgO$ , and  $MgH_2$ . Fig. 4(b)–(f) shows the XRD patterns of the product after 0.5, 3, 5, 10, and 20 h of ball milling, respectively. Peaks of the XRD pattern in Fig. 4(c) are in a good agreement with the characteristic spectrum of  $LaH_3$  crystal,  $MgO$  crystal, and  $MgH_2$  crystal in the JCPDS database. The decrease in intensity of the  $MgH_2$  peaks suggests that  $NaBO_2$  began to react with  $MgH_2$  and formed  $NaBH_4$ . The absence of  $NaBO_2$  peaks in Fig. 4(c) was due to pulverization of

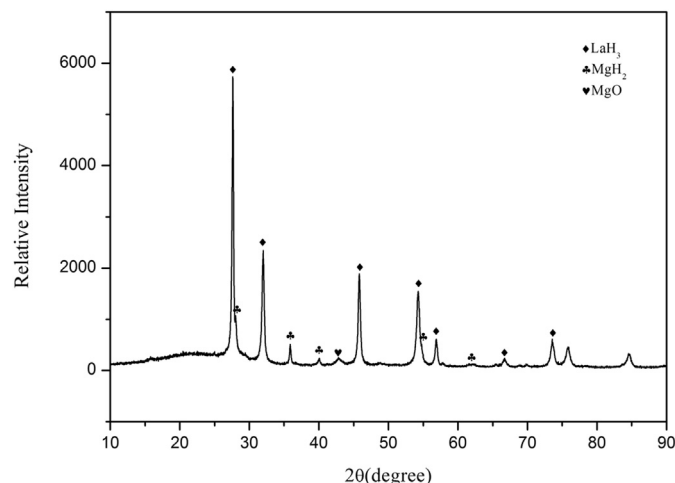


Fig. 3. XRD patterns of hydrogenated  $Mg_3La$ .

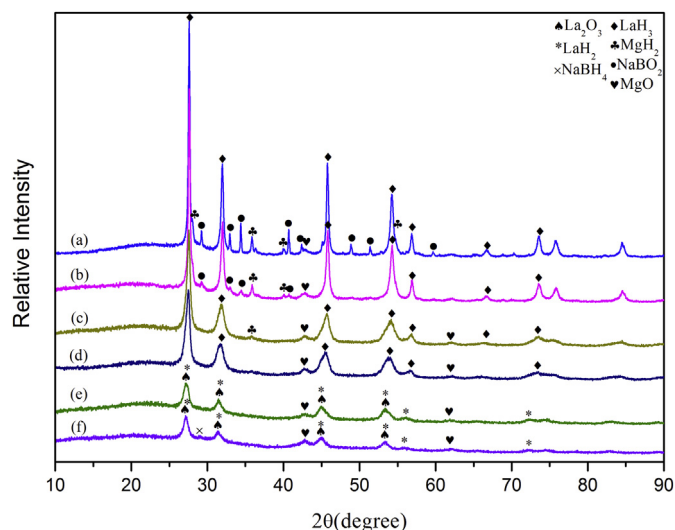
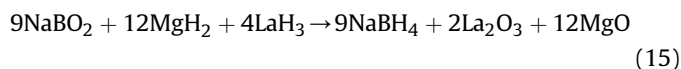


Fig. 4. XRD patterns of (a) the  $NaBO_2$ – $Mg_3La$  hydride mixture and the product after ball milling the  $NaBO_2$ – $Mg_3La$  hydride mixture for (b) 0.5 h (c) 3 h (d) 5 h (e) 10 h (f) 20 h.

$NaBO_2$  particles after ball milling and their participation of the particles in the mechanochemical reaction producing  $NaBH_4$ .

Peaks of the XRD pattern in Fig. 4(d) could be indexed to  $LaH_3$  and  $MgO$ . Peaks corresponding to  $MgH_2$  became indistinguishable and those of  $LaH_3$  broadened. Peaks of the XRD pattern in Fig. 4(e) could be indexed to  $La_2O_3$ ,  $LaH_2$ , and  $MgO$ . After 10 h of milling, peaks corresponding to  $MgH_2$  were absent and those corresponding to  $La_2O_3$  and  $LaH_2$  appeared in the XRD patterns. These changes indicate that initially,  $MgH_2$  reacted completely with  $NaBO_2$ . Part of the  $LaH_3$  reacted with the remaining  $NaBO_2$  to form  $NaBH_4$ , and another part transformed to  $LaH_2$ . The reaction between  $NaBO_2$  and  $LaH_3$  may be expressed as follows:



Products of the above reaction were analyzed by FT-IR spectroscopy. Fig. 5 presents the FT-IR spectrum of the product. As shown in Fig. 5, peaks between  $2200$  to  $2400 \text{ cm}^{-1}$  and at  $1125 \text{ cm}^{-1}$  are due to the B–H stretching and B–H deformation vibrations of pure  $NaBH_4$ , respectively [22]. These peaks confirm

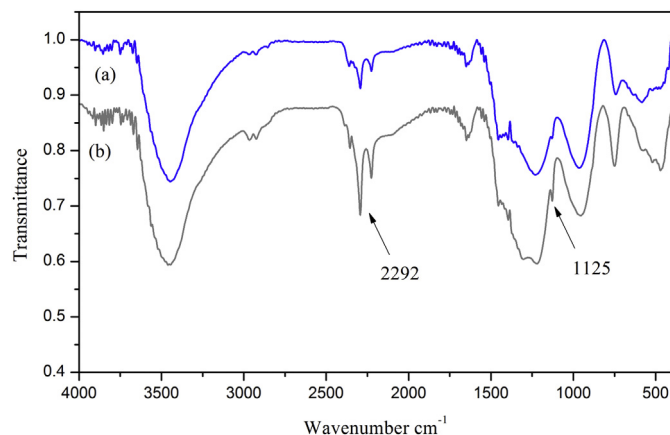


Fig. 5. FT-IR spectrum of the product after ball milling the  $NaBO_2$ – $Mg_3La$  hydride mixture for (a) 5 h (b) 10 h.



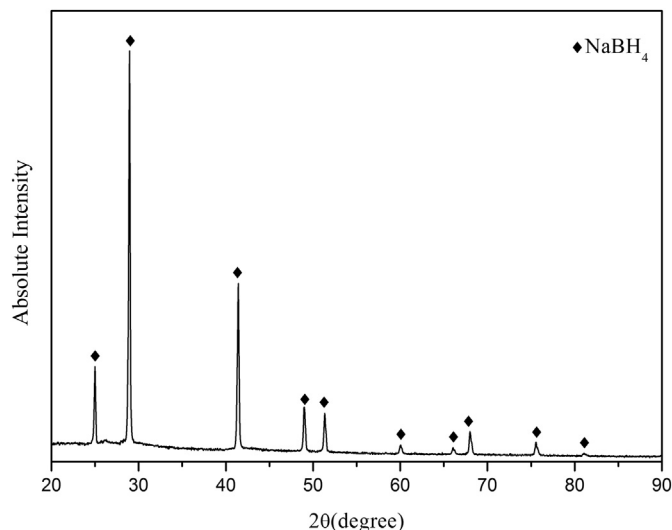


Fig. 6. XRD patterns of the white solid product obtained after purifying.

the reaction of  $\text{H-Mg}_3\text{La}$  with  $\text{NaBO}_2$  to form  $\text{NaBH}_4$ . Peaks of  $\text{NaBH}_4$  are relatively weak and even unidentified. Fig. 4(e) also indicates the amorphization of  $\text{NaBH}_4$  during regeneration. Fig. 4(f) depicts the XRD pattern of the reaction products milled for 20 h. Peaks in this pattern could be indexed to  $\text{LaH}_2$ ,  $\text{La}_2\text{O}_3$ ,  $\text{MgO}$ , and  $\text{NaBH}_4$ . Relatively strong peaks of  $\text{NaBH}_4$  in Fig. 4(f) are due to crystallization of  $\text{NaBH}_4$  after 20 h of milling. XRD patterns of the white solid product obtained after 20 h of milling and purification are shown in Fig. 6. Peaks in this pattern could be indexed to the  $\text{NaBH}_4$  crystal. Thus, these results also prove that  $\text{H-Mg}_3\text{La}$  could react with  $\text{NaBO}_2$  to produce  $\text{NaBH}_4$ .

#### 4. Conclusion

Recycling of  $\text{NaBH}_4$  by  $\text{NaBH}_4$  hydrolysis and  $\text{NaBO}_2$  regeneration using a reaction with  $\text{MgH}_2$ , was examined in the present study. The energy efficiency of the entire recycling process was determined according to thermodynamics calculations. The maximum energy efficiency (49.91%) indicates that reaction of  $\text{MgH}_2$  with  $\text{NaBO}_2$  to form  $\text{NaBH}_4$  during ball milling is feasible. An

inexpensive method of  $\text{NaBH}_4$  regeneration by ball milling was demonstrated by reacting  $\text{H-Mg}_3\text{La}$  with  $\text{NaBO}_2$ .  $\text{Mg}_3\text{La}$ , which could be hydrogenated at room temperature, further improved the energy efficiency. In the reaction of  $\text{H-Mg}_3\text{La}$  with  $\text{NaBO}_2$ ,  $\text{MgH}_2$  reacts with  $\text{NaBO}_2$  completely in the first step and then  $\text{LaH}_3$  reacts with  $\text{NaBO}_2$  to form  $\text{NaBH}_4$ .

#### Acknowledgments

This work was supported by the NBRPC (973 Program No. 2010CB631302), by the National Natural Science Foundation of China Projects (Nos. U1201241 and 51271078), by GDUPS (2014) and by KLGHEI (KLB11003).

#### References

- [1] J. Lu, Z.Z. Fang, H.Y. Sohn, J. Power Sources 172 (2007) 853–858.
- [2] A. Pozio, M.D. Francesco, G. Monteleone, R. Oronzio, S. Galli, C.D. Angelo, et al., Int. J. Hydrogen Energy 33 (2008) 51–56.
- [3] B.H. Liu, Z.P. Li, J. Power Sources 187 (2009) 527–534.
- [4] J. Lee, T. Kim, Sens. Actuators A 177 (2012) 54–59.
- [5] T. Kim, Int. J. Hydrogen Energy 37 (2012) 2440–2446.
- [6] L.Y. Kong, X.Y. Cui, H.Z. Jin, J. Wu, H. Du, T.Y. Xiong, Energy Fuels 23 (2009) 5049–5054.
- [7] C.L. Hsueh, C.H. Liu, B.H. Chen, C. Chen, Y.C. Kuo, K.J. Hwang, J.R. Ku, Int. J. Hydrogen Energy 34 (2009) 1717–1725.
- [8] Y. Kojima, T. Haga, Int. J. Hydrogen Energy 28 (2003) 989–993.
- [9] Ç. Çakanyildirim, M. Gürü, Renew. Energy 35 (2010) 1895–1899.
- [10] B.H. Liu, Z.P. Li, N. Morigasaki, S. Suda, Int. J. Hydrogen Energy 33 (2008) 1323–1328.
- [11] K.S. Eom, E.A. Cho, M.J. Kim, S.K. Oh, S.W. Nam, H.S. Kwon, Int. J. Hydrogen Energy 38 (2013) 2804–2809.
- [12] U.B. Demirci, O. Akdim, P. Miele, Int. J. Hydrogen Energy 34 (2009) 2638–2645.
- [13] L.Z. Ouyang, C.H. Peng, M. Zhu, Int. J. Hydrogen Energy 32 (2007) 3929–3935.
- [14] L.Z. Ouyang, F.X. Qin, M. Zhu, Scr. Mater. 55 (2006) 1075–1078.
- [15] L.Z. Ouyang, H.W. Dong, M. Zhu, J. Alloys Compd. 446–447 (2007) 124–128.
- [16] Ç. Çakanyildirim, M. Gürü, Energy Source Part A 33 (2011) 1912–1920.
- [17] S.C. Amendola, S.L. Sharp-Goldman, M.S. Janjua, M.T. Kelly, P.J. Petillo, M. Binder, J. Power Sources 85 (2000) 186–189.
- [18] P. Wang, A.M. Wang, Y.L. Wang, H.F. Zhang, Z.Q. Hu, Scr. Mater. 43 (2000) 83–87.
- [19] N.A. Lange, J.A. Dean, Lange's Handbook of Chemistry, McGraw-Hill, 1979.
- [20] W. Greiner, L. Neise, H. Stöcker, Thermodynamics and Statistical Mechanics, Springer-Verlag, 1995.
- [21] M.E. Gálvez, A. Frei, G. Albisetti, G. Lunardi, A. Steinfeld, Int. J. Hydrogen Energy 33 (2008) 2880–2890.
- [22] H.P. Zhang, S.Y. Zheng, F. Fang, G.R. Chen, G. Sang, D.L. Sun, J. Alloys Compd. 484 (2009) 352–355.